Mitogen-inducible gene 6 is an endogenous inhibitor of HGF/Met-induced cell migration and neurite growth

Guido Pante,[1] Jane Thompson,[2] Fabienne Lamballe,[3] Tomoko Iwata,[4] Ingvar Ferby,[1] Francis A. Barr,[5] Alun M. Davies,[6] Flavio Maina,[3] and Rüdiger Klein[1]

[1]Department of Molecular Neurobiology, Max Planck Institute of Neurobiology, 82152 Munich-Martinsried, Germany
[2]Fujisawa Institute of Neuroscience, Edinburgh EH8 9JE, Scotland, UK
[3]INSERM UMR 623, Developmental Biology Institute of Marseille, 13288 Marseille, Cedex 09, France
[4]Division of Cancer Sciences and Molecular Pathology, Faculty of Medicine, University of Glasgow, Beatson Laboratories, Bearsden, Glasgow G61 1BD, Scotland, UK
[5]Intracellular Protein Transport Independent Junior Research Group, Max Planck Institute of Biochemistry, 82152 Munich-Martinsried, Germany
[6]School of Biosciences, Cardiff CF103US, Wales, UK

Hepatocyte growth factor (HGF)/Met signaling controls cell migration, growth and differentiation in several embryonic organs and is implicated in human cancer. The physiologic mechanisms that attenuate Met signaling are not well understood. Here we report a mechanism by which mitogen-inducible gene 6 (Mig6; also called Gene 33 and receptor-associated late transducer) negatively regulates HGF/Met-induced cell migration. The effect is observed by Mig6 overexpression and is reversed by Mig6 small interfering RNA knock-down experiments; this indicates that endogenous Mig6 is part of a mechanism that inhibits Met signaling. Mig6 functions in cells of hepatic origin and in neurons, which suggests a role for Mig6 in different cell lineages. Mechanistically, Mig6 requires an intact Cdc42/Rac interactive binding site to exert its inhibitory action, which suggests that Mig6 acts, at least in part, distally from Met, possibly by inhibiting Rho-like GTPases. Because Mig6 also is induced by HGF stimulation, our results suggest that Mig6 is part of a negative feedback loop that attenuates Met functions in different contexts and cell types.

Introduction

The signals that regulate the development of organs need to act for a limited duration in the right place and time. To avoid signaling errors that lead to aberrant cellular behavior and disease, cellular mechanisms have evolved to ensure that appropriate parameters of a signal are received and maintained for the correct time. Hepatocyte growth factor (HGF)/scatter factor acts through the Met receptor tyrosine kinase to mediate a complex process that is called invasive growth (Trusolino and Comoglio, 2002). This process combines cell proliferation with cell–cell dissociation and movement, ECM degradation, and survival. Met-mediated invasive growth plays key roles in placenta, liver, and muscle development, as well as in certain aspects of nervous system development (for review see Maina and Klein, 1999; Birchmeier et al., 2003; see also Helmbacher et al., 2003; Prunotto et al., 2004).

The signaling events that are activated by Met have been well characterized and involve the concomitant activation of the Ras/MAPK and phosphatidyl-inositol 3 (PI3) kinase pathways, in addition to the recruitment and phosphorylation of the multiadaptor, GAB1 (Rosario and Birchmeier, 2003). It seems as if many of the downstream pathways are functionally redundant and extensively cross-wired. However, superimposed above a generic threshold signaling level, specific effectors seem to be required to achieve specific biologic functions (Maina et al., 2001).

Cell migration requires extensive remodeling of the cell cytoskeleton, which is mediated by members of the Rho family of small GTPases (for review see Labouesse, 2004). In their active GTP-bound state, they interact with several effector proteins. Many of these effectors share a common Cdc42-Rac interactive binding (CRIB) domain. CRIB domain–containing effectors are structurally and functionally diverse and include protein kinases, actin binding proteins, and adaptor proteins,

Correspondence to Rüdiger Klein: rklein@neuro.mpg.de

Abbreviations used in this paper: Ack, activated Cdc42-associated tyrosine kinase; Cdc42*, dominant-active Cdc42; CRIB, Cdc42/Rac interactive binding; FGF2, fibroblast growth factor 2; Grb2, growth factor receptor–bound protein 2; HGF, hepatocyte growth factor; LacZV5, V5 epitope–tagged β-galactosidase; Mig6, mitogen-inducible gene 6; $Mig6^{FL}$, full-length Mig6; $Mig6^{FL\text{-}V5}$, SDF-1, stromal cell–derived factor 1; V5 epitope–tagged versions of Mig6; PI3, phosphatidyl-inositol 3; siRNA, small interfering RNA.

The online version of this article contains supplemental material.

The Journal of Cell Biology, Vol. 171, No. 2, October 24, 2005 337–348
http://www.jcb.org/cgi/doi/10.1083/jcb.200502013

such as mitogen-inducible gene 6 (Mig6; see below next paragraph) (for review see Pirone et al., 2001).

Signaling by receptor tyrosine kinases requires a counterbalance by negative signaling events to ensure that appropriate thresholds of receptor signals are achieved and maintained for the right length of time. Irreversible inhibition is mediated most commonly by activation-dependent protein degradation through the ubiquitin–proteasome pathway. Reversible inhibition can be achieved by protein tyrosine phosphatases, by dual-specificity MAPK phosphatases, and by phosphatase and tensin homologue proteins, which down-regulate the PI3 kinase pathway (Dikic and Giordano, 2003).

In a screen for HGF-induced changes in the transcriptome of cultured cells, we identified the Mig6 adaptor protein in a set of highly induced transcripts. Mig6 (also known as Gene 33 and receptor-associated late transducer) is considered an immediate early response gene that can be induced by a variety of external stimuli, including growth factors, cytokines, and stress factors (Wick et al., 1995; Makkinje et al., 2000; and references within). Overexpression and knock-down studies suggested that Mig6 was a selective inhibitor of EGF receptor family (also known as ErbB receptors)–mediated mitogenesis and transformation (Fiorentino et al., 2000; Hackel et al., 2001; Fiorini et al., 2002; Anastasi et al., 2005; Xu et al., 2005). Its mechanism of action, receptor specificity, and influence on other cellular activities are poorly understood or unknown.

Here we show that Mig6 is a negative regulator of HGF/Met-induced cell migration. The effect was observed by Mig6 overexpression and was reversed by Mig6 small interfering RNA (siRNA) knock-down experiments, which indicates that endogenous Mig6 is part of a mechanism that inhibits Met signaling. The effect is observed in cells of hepatic origin as well as in primary neurons; this suggests that Mig6 functions across different cell lineages. Met lacks the sequence identified in EGF receptor as the Mig6 binding region (Hackel et al., 2001) and fails to bind Mig6 directly. Instead, Mig6 requires an intact CRIB domain to exert its inhibitory action, and suggests that Mig6 acts, at least in part, distal from the receptor, possibly by interacting with Rho family GTPases. Because Mig6 also is induced by HGF stimulation, our results suggest that Mig6 is part of a negative feedback loop that attenuates Met signaling in a variety of cellular functions.

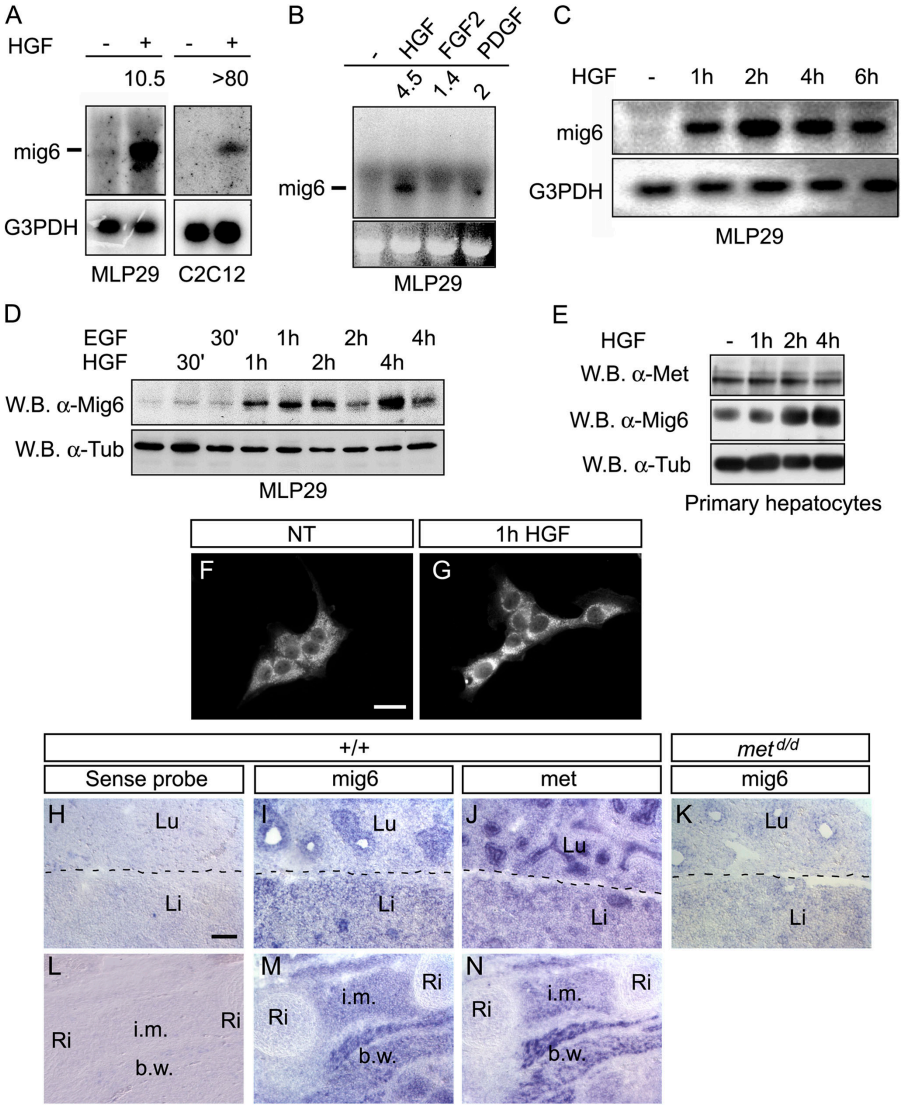

Figure 1. **Induction of Mig6 by HGF/Met signaling in cultured cells and coexpression of Mig6 with Met in vivo.** (A–C) Northern blot analysis showing mig6 mRNA up-regulation upon HGF, FGF, or PDGF stimulation for 4 h (A and B) or the indicated times (C) in MLP29 and C2C12 cells. 18S or glyceraldehyde 3–phosphate dehydrogenase (G3PDH) mRNA levels were used as internal control. Western blot (W.B.) analysis showing Mig6 protein induction upon HGF and EGF stimulation in MLP29 cells (D) and primary hepatocytes (E). Cells were grown in 10% FBS, then stimulated with empty media, 40 ng/ml HGF, or 10 ng/ml EGF for the indicated times, lysed, and analyzed by SDS-PAGE and immunoblotting using a specific anti-Mig6 antiserum. Immunoblots for α-tubulin and Met were used as internal controls. Immunocytochemistry analysis showing Mig6 protein induction upon HGF stimulation in MLP29 cells. Cells stimulated as above with empty media (F) or with HGF (G), fixed, and stained using a specific anti-Mig6 antiserum. NT, not treated. Bar, 50 μm. (H–N) In situ hybridization analyses for mig6 and met mRNA transcripts in selected organs of E13.5 wild-type ($^{+/+}$) and Met signaling–deficient ($met^{d/d}$) embryos. Co-expression of mig6 and met is observed in alveoli of the lungs (Lu), liver (Li), intercostal muscle (i.m.), and body wall muscle (b.w.) (I, J, M, and N). Mig6 transcript levels are reduced in $met^{d/d}$ embryo lungs and liver (K). Mig6 sense probe was used as negative control on adjacent sections (H, L). Ri, ribs. Bar, 300 μm.

Results

Mig6 induction by HGF/Met signaling

Part of our efforts to understand the molecular events that control HGF/Met signaling has been to examine the expression of genes that are regulated by Met signaling. RNA from HGF-stimulated and unstimulated MLP29 cells, a liver-derived cell line that expresses physiologic levels of Met (Medico et al., 1996), was subjected to microarray analysis (Tanaka et al., 2000). Genes that showed >1.8-fold changes and whose sum of median value was >5,000 were included in the final list. Expression levels of ~100 genes were up-regulated, whereas ~30 genes were down-regulated by HGF stimulation in MLP29 cells (Tables SI and SII; available at http://www.jcb.org/cgi/content/full/jcb.200502013/DC1). Analysis, by Northern blotting, of selected candidates on two independent cell lineages (MLP29 hepatic cells and C2C12 myoblast cells) confirmed Met-mediated regulation of most hits from the microarray analysis (Fig. S1 A).

Mig6 was chosen for further analysis because its expression was induced more strongly by HGF—4.5- to 80-fold by 4 h of HGF stimulation—than by fibroblast growth factor 2 (FGF2) or PDGF (Fig. 1, A and B). Other transcripts did not show this preference for HGF (Fig. S1 B). The reduced response to FGF2 and PDGF was not due to lack of specific receptors or downstream transducers, because both growth factors induced robust phosphorylation of ERK/MAPKs in MLP29 cells (Fig. S2; available at http://www.jcb.org/cgi/content/full/jcb.200502013/DC1). Time courses of HGF stimulation revealed that Mig6 mRNA and protein were induced half maximally after 1 h and maintained for several hours (Fig. 1, C and D). The induction of Mig6 protein by EGF was more transient than that induced by HGF (Fig. 1 D). Induction of Mig6 protein by HGF in primary hepatocytes followed delayed kinetics (Fig. 1 E). We also confirmed the induction of endogenous Mig6 protein by immunostaining of MLP29 cells (Fig. 1, F and G). We next investigated the expression of Mig6 and Met in embryonic tissues. By in situ hybridization analysis, we found that both transcripts coexpressed in alveoli of

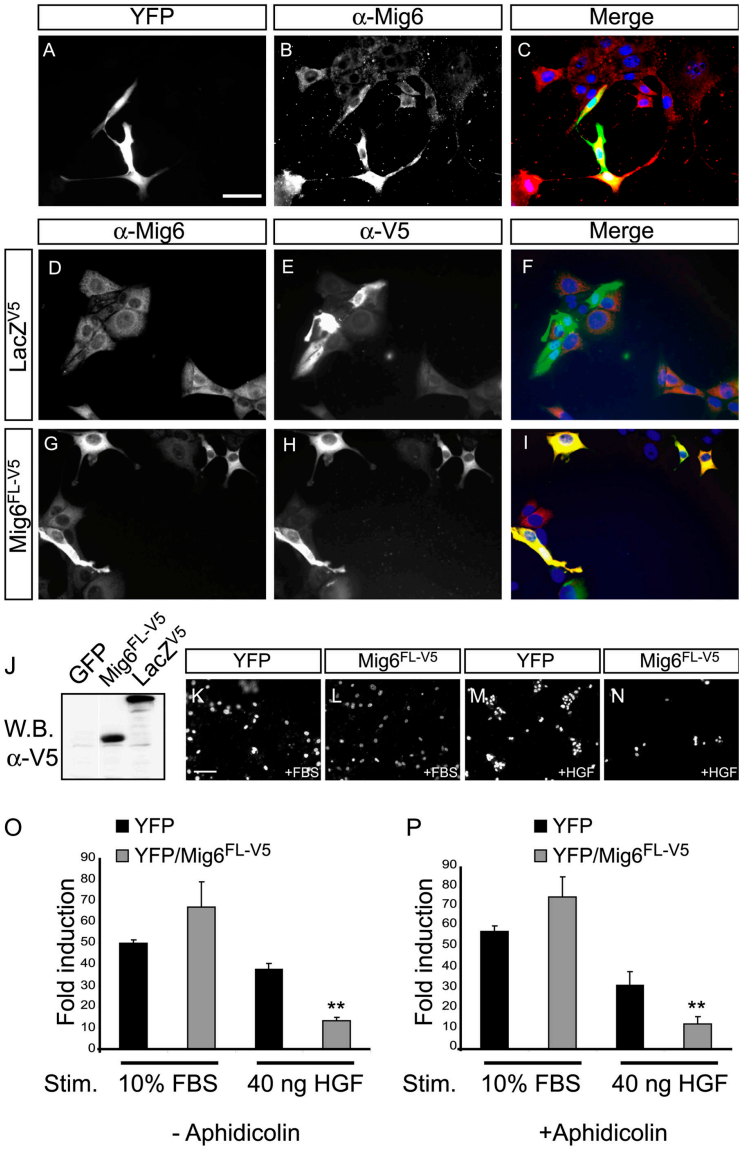

Figure 2. **Mig6 overexpression inhibits HGF-mediated cell migration.** (A–C) MLP29 cells were transfected with a mixture of YFP and $Mig6^{FL-V5}$ expression plasmids in a ratio of 1:5. 24 h later, cells were starved in 0.1% FBS for an additional 24 h, harvested, and seeded onto coverslips for immunocytochemical analysis. Cells were fixed and Mig6 overexpression was detected using a Mig6-specific antibody (B). YFP-expressing cells (A) are strongly positive for Mig6 (C). Bar, 50 μm. (D–I) MLP29 cells were transfected with $Mig6^{FL-V5}$ or $LacZ^{V5}$ expression plasmids and stained with anti-Mig6 and anti-V5 antibodies as above. $LacZ^{V5}$ transfected cells were weakly positive for (endogenous) Mig6 and strongly positive for the V5 epitope (D–F). $Mig6^{FL-V5}$ transfected cells showed strong costaining for Mig6 and V5 (G–I) indicating efficient overexpression of Mig6. (J) Western blot (W.B.) using V5 antibodies to detect $Mig6^{FL-V5}$ or $LacZ^{V5}$ expression. (K–N) Photographs of Hoechst dye–labeled cells after migration through the Boyden chamber membrane. Cells were transfected with the indicated expression plasmids as described above, and a portion was seeded onto the upper face of the membrane. Cells were exposed to 10% FBS (K and L) or 40 ng/ml HGF (M and N). Reduced migration due to Mig6 overexpression was observed in the YFP-positive (see quantification below) and in the total Hoechst dye–positive cell population (compare M with N). Bar, 100 μm. Quantification of migration of YFP-expressing cells indicated as fold of induction over unstimulated cells, in the absence (O) or presence (P) of the DNA polymerase inhibitor, aphidicolin. Mig6 overexpression reduced HGF-stimulated cell migration by approximately threefold in the absence (O; $P < 0.001$, *t* test) or presence of aphidicolin (P; $P < 0.001$, *t* test). In contrast, cell migration stimulated (Stim.) with 10% FBS in the absence or presence of aphidicolin was unaffected by Mig6 overexpression ($P = 0.45$ and $P = 0.121$, respectively; *t* test).

embryonic (E13.5) lung, in liver parenchyma, and in intercostal and body wall muscles of wild-type embryos (Fig. 1, I, J, M, and N). Consistent with Met regulating mig6 transcript levels under physiologic conditions, we found reduced levels of mig6 mRNA in embryos that expressed a signaling-deficient Met receptor ($met^{d/d}$) (Maina et al., 1996, 2001) (Fig. 1 K). Expression of Mig6 protein was confirmed in structures positive for *mig6* mRNA, including intercostal and body wall muscles (Fig. S2).

Overexpression of Mig6 inhibits HGF-induced migration of MLP29 cells

The only cellular context in which Mig6 has been implicated is cell division. However, because HGF/Met signaling is critical for cell migration, we tested the effects of Mig6 overexpression on HGF/Met-mediated migration in the Boyden chamber migration assay. This assay tests the capacity of cells to migrate through a porous membrane that separates upper and lower compartments. MLP29 cells were transfected with a plasmid that encodes YFP, or cotransfected with plasmids that encode full-length Mig6 ($Mig6^{FL}$) and YFP (Fig. 2, A–C). We confirmed the expression of exogenous Mig6 by immunostaining of cells and immunoblotting of lysates from cells expressing V5 epitope–tagged versions of Mig6 ($Mig6^{FL\text{-}V5}$) in comparison with V5 epitope–tagged β-galactosidase ($LacZ^{V5}$) (Fig. 2, D–J). For each experimental condition, equal numbers of cells were seeded onto coverslips for immunocytochemical analysis, or onto the upper compartment of the Boyden chamber and were exposed to varying concentrations of HGF or 10% FBS in the lower compartment. Cell migration through the membrane into the lower compartment was stimulated by HGF in a dose-dependent manner (unpublished data). At 40 ng/ml HGF, migration of transfected, YFP-positive cells was enhanced 30- to 40-fold over unstimulated cells (Fig. 2, O and P). Representative images of Hoechst dye–labeled cells, which migrated into the lower compartment of the Boyden chamber, are shown in Fig. 2 (K–N). The presence of $Mig6^{FL}$ reduced HGF-stimulated cell migration by approximately threefold (Fig. 2 O, $P < 0.001$, *t* test). In contrast, cell migration that was stimulated with 10% FBS was unaffected by Mig6 overexpression ($P = 0.121$, *t* test).

Because Mig6 overexpression also reduced cell proliferation that was induced by HGF (unpublished data), we next asked whether the effect on cell migration could be secondary to reduced cell proliferation. Transfected cells were exposed to 1.6 μg/ml of the DNA polymerase inhibitor, aphidicolin, 24 h before plating onto the membrane; the assay was conducted in the presence of 1.6 μg/ml aphidicolin. Typically, aphidicolin treatment reduced the incorporation of BrdU into MLP29 cells 10-fold (unpublished data). Under these conditions, HGF-stimulated cell migration still was reduced significantly by Mig6 overexpression which indicated that Mig6 had a direct influence on Met-mediated cell migration, independently of its effect on cell proliferation (Fig. 2 P; $P < 0.01$, *t* test).

Mig6 is a physiologic suppressor of Met-mediated cell migration

We next investigated, using RNA interference, whether endogenous Mig6 suppressed HGF/Met-mediated cell migration by

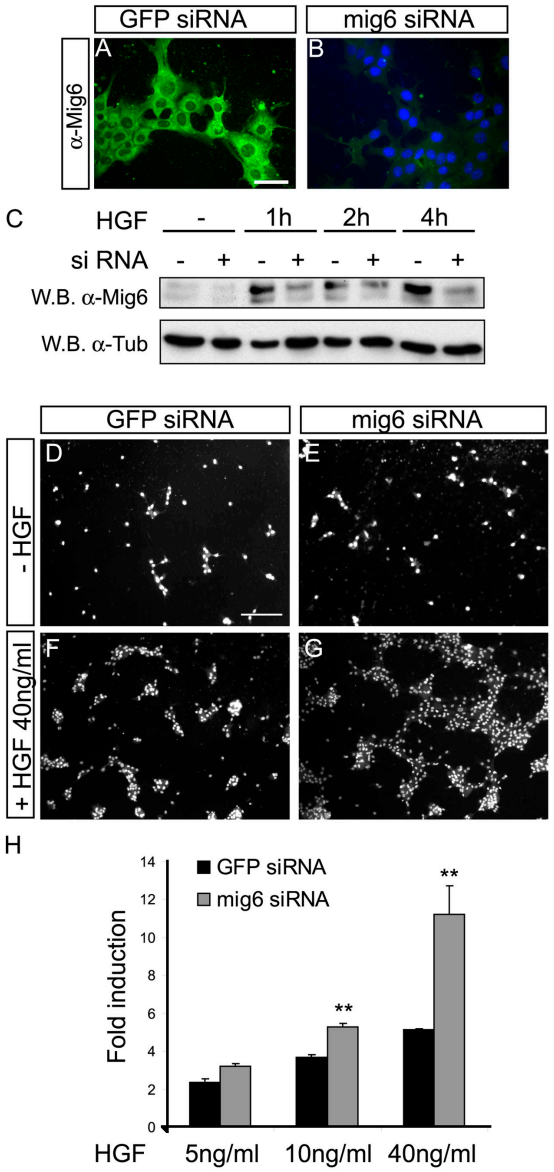

Figure 3. **Endogenous Mig6 inhibits HGF-induced cell migration in MLP29 cells.** MLP29 cells were transfected with GFP-specific siRNAs as a negative control (A) or with mig6-specific siRNAs (B) for 4 d, then fixed, and Mig6 protein levels were detected by immunofluorescence using a Mig6-specific antibody (green label). (B) Cells were visualized using Hoechst dye. Note the efficient knock-down of Mig6 protein levels upon transfection of mig6 siRNAs. Bar, 50 μm. (C) Western blot (W.B.) analysis of MLP29 cells transfected with GFP siRNAs (−) or mig6-specific siRNAs (+) for 4 d. After transfection, the cells were stimulated with 40 ng/ml HGF for the indicated times and the cell lysates were analyzed using SDS-PAGE and immunoblotting using α-Mig6– or α-tubulin–specific (α-Tub) antibodies. The specific reduction of Mig6 levels is seen most clearly at the 4-h time point. (D–G) Representative fields of GFP siRNA– and mig6 siRNA–transfected MLP29 cells (labeled with Hoechst dye) that migrated into the lower compartment of the Boyden chamber in the presence or the absence of HGF. MLP29 cells were treated as described above, then transfected a second time with siRNA oligonucleotides, incubated for 24h, harvested, plated into the upper compartment of the Boyden chamber, and allowed to attach onto the membrane. Different concentrations of HGF were added to the media of the lower compartment of the chamber and the cells were allowed to migrate for 16 h. Note the increase of cell migration of mig6 knock-down cells after HGF stimulation (compare panels F and G). Bar, 100 μm. (H) Quantification of migration expressed as fold of induction over unstimulated cells. Increasing concentrations of HGF were added to the lower chamber after transfection of control GFP siRNAs (black bars) or mig6 siRNAs (gray bars). 5 ng/ml HGF, $P = 0.02$; 10 ng/ml HGF, $P < 0.0002$; 40 ng/ml HGF, $P < 0.01$, *t* test.

knocking down Mig6 protein levels (Elbashir et al., 2001). MLP29 cells were transfected with siRNAs specific for GFP or mig6, and the levels of Mig6 protein were analyzed by immunostaining and immunoblotting. Mig6 siRNA, but not control GFP siRNA, specifically knocked down endogenous Mig6 immunoreactivity 96 h after transfection (Fig. 3, A and B). Mig6 siRNA also suppressed HGF-stimulated induction of Mig6 (Fig. 3 C; compare 4-h time point in the presence and absence of mig6 siRNA). The reduction of protein levels was specific for mig6, because endogenous α-tubulin and Met levels were unaffected (Fig. 3 C and not depicted). To investigate the role of Mig6 protein in cell migration, cells were transfected with mig6 siRNA oligonucleotides, and subjected to the Boyden chamber assay with different concentrations of HGF (Fig. 3). Representative images of Hoechst dye–labeled cells that migrated into the lower compartment are shown in Fig. 3 (D–G). The induction of cell migration by HGF under these conditions was less strong, yet was still dose dependent (Fig. 3 H). Quantification of migrating cells revealed that under conditions of optimal HGF concentrations, knock down of Mig6 enhanced cell migration by approximately twofold (Fig. 3 H). Similar results were obtained with a separate set of siRNA oligonucleotides (unpublished data). These findings demonstrated that Mig6 is a physiologic inhibitor of HGF/Met-mediated cell migration of MLP29 cells.

Knock-down of Mig6 also enhanced MLP29 cell proliferation (unpublished data), as previously shown in EGF-stimulated fibroblasts (Xu et al., 2005). To separate Mig6's effects on cell proliferation from cell migration, we assayed cell migration in the presence of the cell cycle inhibitor, aphidicolin. In the presence of DMSO-containing control media, knock-down of Mig6 protein levels led to a significant increase in HGF-induced cell migration (Fig. 4, A, B, and E). This effect was not diminished by the presence of aphidicolin, if anything, it was enhanced slightly (Fig. 4, C–E). These data indicate that endogenous Mig6 blocks cell migration independently of its antiproliferative effects.

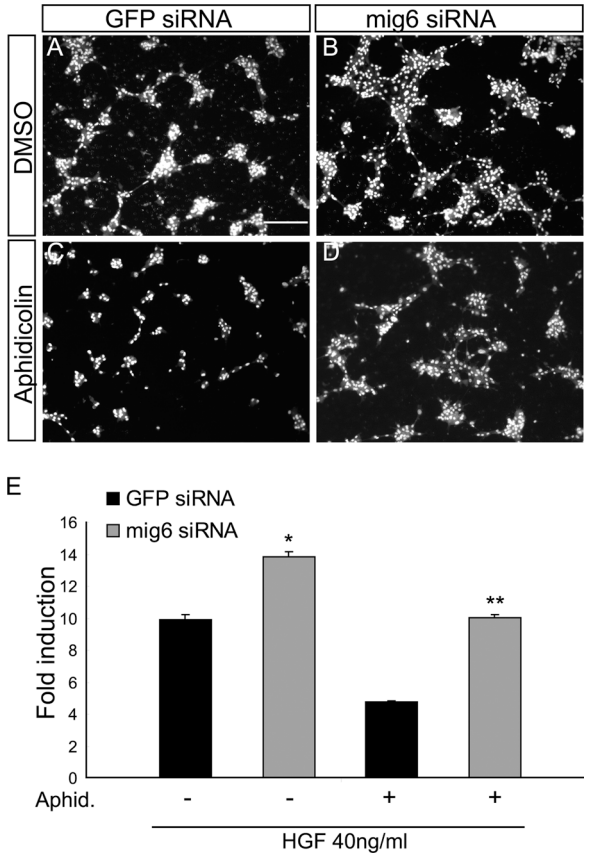

Figure 4. **Physiologic inhibition of HGF-mediated cell migration by Mig6 is independent of its effects on proliferation.** Representative Hoechst dye–labeled MLP29 cells that were transfected with GFP-specific siRNAs (A and C) or Mig6-specific siRNAs (B and D) migrated onto the lower face of the Boyden chamber membrane upon stimulation with HGF. The cells were exposed to media containing DMSO (A and B) or 1.6 μg/ml aphidicolin solubilized in DMSO (C and D). Bar, 100 μm. (E) Quantification of cell migration expressed as fold of induction over unstimulated cells. Migration was enhanced in cells transfected with Mig6 siRNAs (gray bars) compared with GFP siRNAs (black bars) in the absence or presence of aphidicolin (Aphid.) ($P = 0.019$ and $P < 0.0002$, respectively, *t* test). *, $P < 0.05$; **, $P < 0.01$.

Cortical neuron migration induced by HGF is sensitive to overexpression of Mig6

We next asked whether the functions of Mig6 were specific to cells of hepatic origin, or whether Mig6 had a more general role in controlling cell migration across different cell lineages, including neurons from the neocortex (Powell et al., 2001). To test the consequences of Mig6 overexpression, embryonic cortical neurons were transfected with a $Mig6^{FL\text{-}V5}$ construct, and Mig6 expression was monitored by immunofluorescence microscopy (Fig. 5, D–G). Our modified electroporation protocol (see Materials and methods) led to transfection efficiencies of 40–70%, as judged by GFP fluorescence (Fig. 5 A). Mig6 overexpression did not affect survival (unpublished data) or differentiation of cortical neurons as judged by the expression of microtubule-associate protein 2 (Fig. 5 B,C). HGF-induced cell migration was assayed 36 h after transfection of expression plasmids that encoded GFP or $Mig6^{FL\text{-}HIS}$. Quantification of all (transfected and untransfected) cells on the lower face of the porous membrane revealed a three- to fourfold increase of migrated cells in the presence of HGF, and a seven- to eightfold stimulation among the GFP transfectants (Fig. 5 H). In contrast, overexpression of Mig6 completely prevented HGF from inducing cell migration (Fig. 5 H). In a separate set of experiments, we compared cells that were transfected with plasmids that encoded $Mig6^{FL\text{-}V5}$ or $LacZ^{V5}$ in the absence or presence of HGF. 24 h after transfection, $LacZ^{V5}$ control cells responded to HGF with a six- to sevenfold higher migration rate (Fig. 5 I). In contrast, $Mig6^{FL\text{-}V5}$-expressing cells failed to migrate (Fig. 5 I; $P < 0.0001$, *t* test). The effect of Mig6 on HGF-induced cell migration was specific, because Mig6 was unable to block cell migration in response to the chemokine stromal cell–derived factor-1 (SDF-1) (Fig. 5 I; $P > 0.28$, *t* test).

Mig6 suppresses HGF/Met-mediated neurite growth

Besides regulating cell migration, HGF is a chemoattractant and neurite growth-promoting factor for subsets of neurons, including sympathetic neurons (Maina and Klein, 1999; Thompson et al., 2004). We next tested the effects of Mig6 on neurite

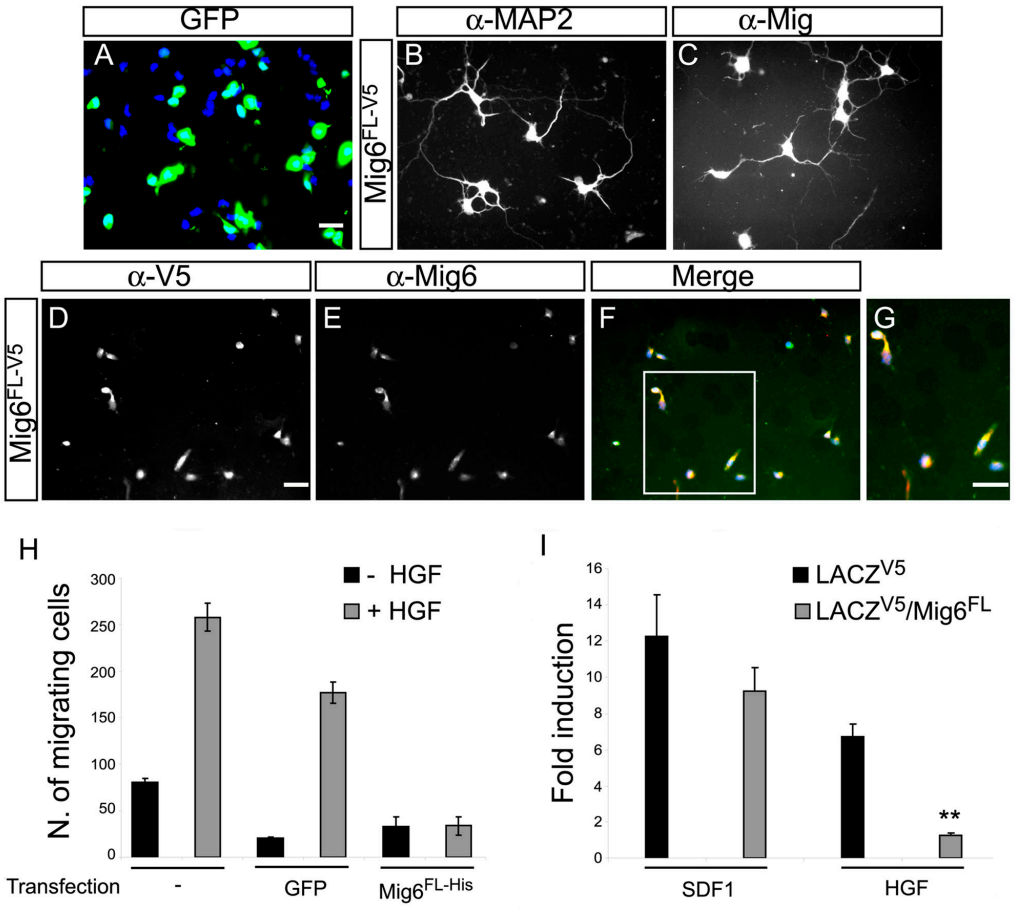

Figure 5. **Mig6 overexpression in cortical neurons inhibits HGF-induced migration.** Cortical neurons were dissected from E15.5 mouse embryos and electroporated with expression plasmids encoding GFP (A) or Mig6$^{FL\text{-}V5}$. Electroporated cells were plated for 24 h (A, D–F) or 3 d (B and C) onto coverslips for immunocytochemical analysis. (A) GFP fluorescent cells (green) among untransfected Hoechst dye–labeled cells. (B and C) After transfection with Mig6$^{FL\text{-}V5}$, cells were cultured for 3 d and immunostained with α-microtubule-associated protein 2 (α-MAP2) (B) or α-Mig6 (α-Mig) antibodies (C). Mig6 did not affect neuronal differentiation. (D–G) Cells were fixed and doubly labeled using α-V5 (D) and α-Mig6 (E) antibodies. Nearly all V5-labeled cells also express Mig6. Similar results were obtained with a HIS-epitope–tagged Mig6 expression plasmid (not depicted). (H) Quantification of Hoechst dye–labeled cortical neurons that have migrated onto the lower face of the Boyden chamber membrane. Cells were left nonelectroporated (−) or were electroporated with expression plasmids encoding GFP or with Mig6$^{FL\text{-}HIS}$. Neurons were seeded onto the upper compartment of the Boyden chamber in the absence (black bars) or presence (gray bars) of 50 ng/ml HGF. The cells were fixed and counted after 24 h. The expression of Mig6$^{FL\text{-}HIS}$ completely prevented HGF-mediated cell migration. (I) Quantification of migrating cortical neurons expressed as fold of induction over unstimulated cells. Cells were electroporated with LacZ^{V5} control or Mig6$^{FL\text{-}V5}$ expression plasmids in the presence of 50 ng/ml HGF or 100 ng/ml SDF-1. Mig6$^{FL\text{-}V5}$ inhibited HGF-induced ($P < 0.0001$, *t* test), but not SDF-1–induced, cell migration ($P > 0.28$, *t* test). Bar, 50 μm.

growth of paravertebral sympathetic neurons. Most postnatal day 40 sympathetic neurons of the superior cervical ganglion survive in culture without addition of neurotrophic factors (unpublished data). Exogenous HGF induced Mig6 expression (Fig. 6 A), and stimulated outgrowth and branching of neurites. To quantify this effect, we transfected the cells with an expression plasmid that encoded YFP by way of gene gun, and used Sholl analysis (see Materials and methods) to determine neurite complexity. HGF (10 ng/ml) significantly increased neurite complexity and branching as compared with nontreated control cultures (Fig. 6, D and F). The effect was most pronounced close to the soma, whereas there was no significant increase in complexity in the longest neurites (Fig. 6 D). To investigate neurite complexity, we compared the neurite arbors of cells that were transfected with expression vectors encoding Mig6 plus YFP with cells expressing YFP alone (Fig. 6, B and C). Overexpression of Mig6 greatly reduced neurite outgrowth and branching of HGF-stimulated cells (Fig. 6 E). The effect was most pronounced close to the cell soma, where HGF had its strongest effects in comparison with control cDNAs, such as YFP (Fig. 6 E). This effect was specific for HGF-treated neurons, because in untreated neurons, expression of Mig6 did not cause a reduction of branch points (Fig. 6 F). Exogenous Mig6 also did not affect survival of HGF-treated neurons, which suggests that Mig6 specifically inhibited Met signaling toward neurite growth (Fig. 6 G). We next performed Mig6 knockdown experiments and found a modest increase in neurite length in Mig6 siRNA-treated, as compared with GFP siRNA-treated, cells. The increase in Mig6 knock-down cells was significant in neurites that extended furthest from the soma. Because the induction of endogenous Mig6 protein is delayed (see Fig. 6 A), the effect of knocking down mig6 mRNA may be

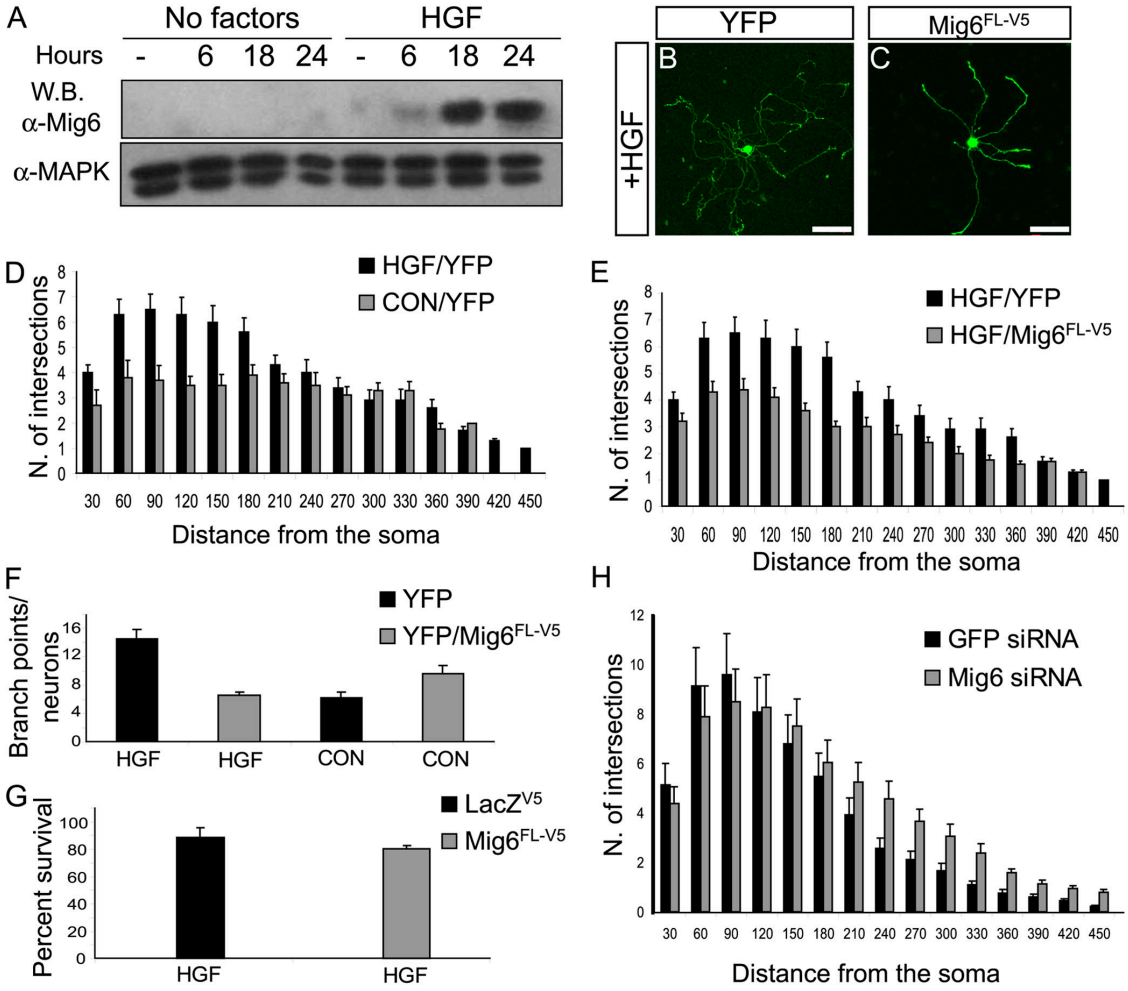

Figure 6. **Mig6 inhibits HGF-induced neurite outgrowth and branching of sympathetic neurons.** (A) Western blotting (W.B.) using an α-Mig6 antibody showing the time course of endogenous Mig6 protein induction upon HGF stimulation in postnatal day 40 (P40) superior cervical ganglion (SCG) neurons (top panel). The α-MAPK antibody was used as internal control. Representative P40 SCG neurons transfected with YFP (B) or with a mixture of YFP plus Mig6^{FL-V5} expression plasmids (C). Cells were grown in medium supplemented with 10 ng/ml HGF for 48 h. Note the significant reduction in neurite complexity of the Mig6^{FL-V5}-expressing cell compared with YFP control. (D) Sholl analysis (see Materials and methods) of P40 SCG neurons transfected with YFP alone and exposed for 48 h to control media (CON/YFP) or 10 ng/ml HGF (HGF/YFP). (E) Sholl analysis of P40 SCG neurons stimulated with 10 ng/ml HGF after being transfected with YFP (black bars) or YFP plus Mig6^{FL-V5} (gray bars). Mig6^{FL-V5} expression was able to block HGF-induced neurite outgrowth completely (compare panels D and E, gray bars). (F) Numbers of neurite branch points per neuron in different experimental conditions. P40 SCG neurons were treated as described above, and the numbers of branch points per neuron were counted in the presence (HGF) or absence (CON) of 10 ng/ml HGF. (G) Percentage of surviving P40 SCG neurons in different experimental conditions. After 48 h of HGF exposure, the neurons were transfected with the control LACZ^{V5} or the Mig6^{FL-V5} expression plasmids. Upon stimulation with HGF, the expression of Mig6^{FL-V5} did not affect P40 SCG neuron survival. (H) Sholl analysis of P40 SCG neurons transfected with Mig6-specific or GFP-specific siRNA oligonucleotides together with an expression plasmid encoding YFP in the presence of 10 ng/ml HGF. Endogenous Mig6 knock-down by siRNA induced a modest increase in neurite branching. Distances in D, E, and H measured in μm.

visible only in the longest neurons that took the most time to grow. These results suggest that Mig6 plays a role in suppressing neurite complexity that is induced by HGF/Met signaling.

The CRIB domain of Mig6 is required for and sufficient to inhibit HGF-mediated cell migration

Mig6 was proposed to inhibit EGFR signaling by direct binding to EGFR and ErbB2—by suppressing the EGFR kinase activity—and by a receptor distal mechanism (Anastasi et al., 2003). To begin dissecting the mechanism of Mig6-mediated inhibition of cell migration, we asked whether Mig6 would directly bind Met in MLP29 cells that were stimulated with HGF. In pull-down experiments that used bacterially expressed, GST-tagged, purified, full-length Mig6, we were unable to demonstrate a direct association between Mig6 and Met (unpublished data). Moreover, the minimal region that was mapped in EGFR to be essential for the binding of Mig6 is not found in the amino acid sequence of mouse Met. However, pull-down experiments with GST-tagged Mig6 confirmed the association with growth factor receptor–bound protein 2 (Grb2) (Fig. 7 A), which had been observed previously (Fiorentino et al., 2000). Control pull-downs with the GST-tagged CRIB domain of P21-associated serine/threonine kinase failed to pull down Grb2 (Fig. 7 A). This suggested the possibility that Mig6 may bind Met indirectly by way of Grb2, thereby inhibiting Met in a receptor-proximal fashion.

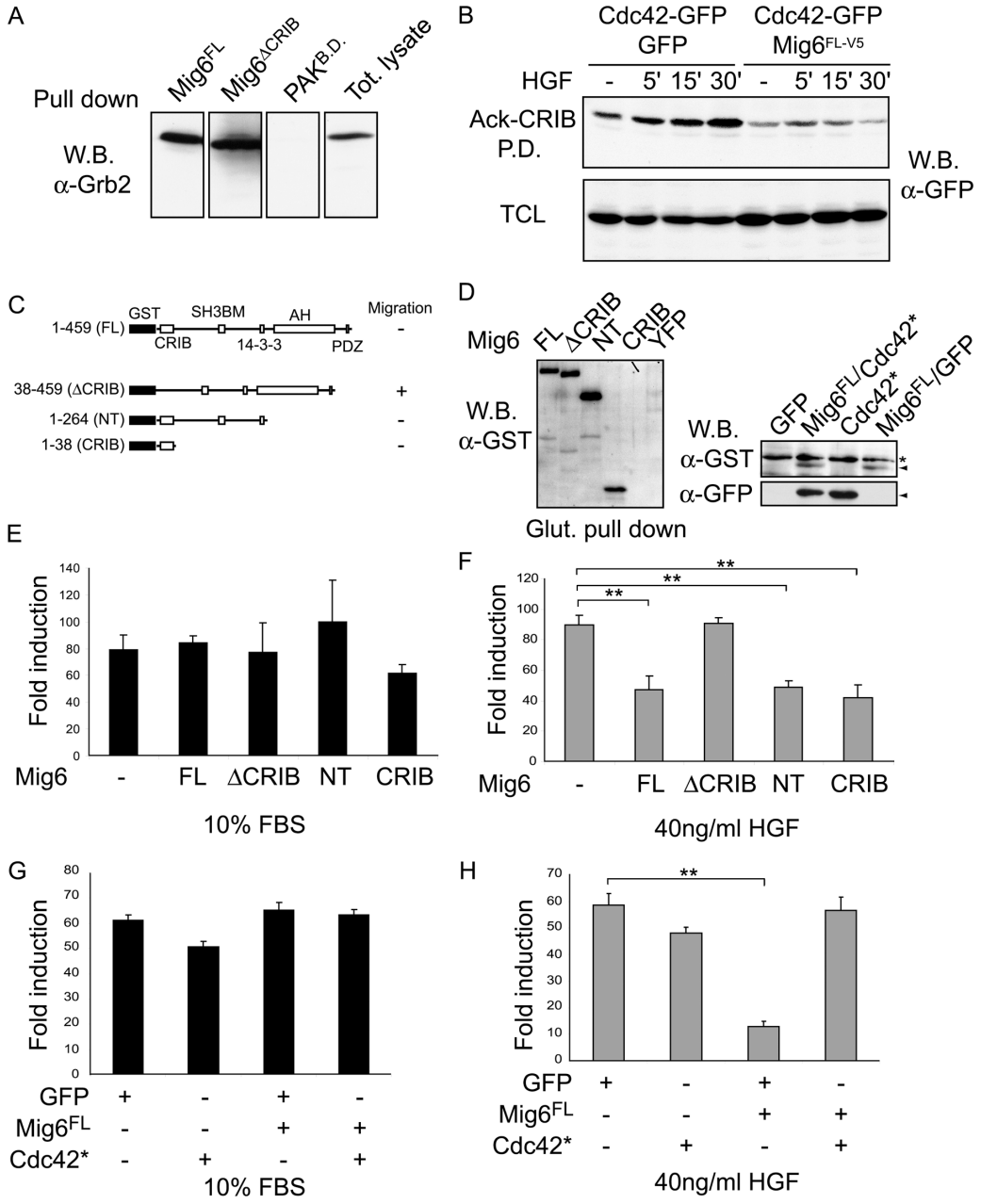

Figure 7. **The CRIB domain of Mig6 is necessary and sufficient to inhibit HGF-induced cell migration.** (A) Mig6 binds Grb2. GST-Mig6^{FL} and GST-Mig6$^{\Delta CRIB}$ purified fusion proteins were used to pull down endogenous Grb2 from MLP29 total cell lysate. The fusion proteins were incubated for 1 h with total (Tot.) cell lysate and pulled down using glutathione-sepharose beads. Pulled-down proteins were eluted from the beads and analyzed by SDS-PAGE. Western blot (W.B.) analysis using an α-Grb2 antibody shows that Grb2 associates with Mig6, and that the association is independent of Mig6's CRIB domain. A GST-PAK^{BD} fusion protein was used as a negative control. (B) Mig6 reduces the levels of Cdc42-GTP. The GST-Ack-CRIB–purified fusion protein was used to pull down (P.D.) the active form (GTP-bound) of transfected GFP-Cdc42 at different time points of HGF stimulation in the presence or the absence of Mig6 expression plasmid. MLP29 cells were transfected with GFP-Cdc42 plus GFP (left half) or GFP-Cdc42 plus Mig6$^{FL\text{-}V5}$ expression plasmids (right half), starved for 48 h in 0.1% FBS, stimulated with 40 ng/ml of HGF for the indicated times, and lysed. The GST-Ack-CRIB protein was incubated with the cell lysates, pulled down using glutathione-sepharose beads, eluted from the beads, and analyzed by SDS-PAGE. Western blot (W.B.) analysis using an anti-GFP–specific antibody showed that exogenous GFP-Cdc42 is activated upon 15 and 30 min (') of HGF stimulation. The expression of Mig6 significantly reduced exogenous GFP-Cdc42 activation upon HGF stimulation (compare 15- and 30-min time points, left and right part of the blot). Western blot analysis on total cell lysates (TCL) using an anti-GFP–specific antibody was used to control that comparable amounts of total GFP-Cdc42 were used for the pull down. (C) Schematic representation of the different GST-Mig6 deletion mutants. 14-3-3, 14-3-3 binding region; AH, Ack homology domain; PDZ, PDZ target site; SH3BM, SH3 binding site. (D, left blot) GST-Mig6^{FL}, GST-Mig6$^{\Delta CRIB}$, GST-Mig6^{NT}, and GST-Mig6^{CRIB} were transfected in MLP29 cells and pulled down using glutathione-Sepharose beads (Glut.). The proteins were eluted from the beads and analyzed by SDS-PAGE. Western blot (W.B.) analysis using an α-GST antibody shows that the Mig6 fusion proteins were expressed at similar levels. Transfection with YFP expression plasmid was used as a negative control for the α-GST antibody. (D, right blot) GST-Mig6^{FL} plus GFP-Cdc42*, GFP-Cdc42*, or GST-Mig6^{FL} plus GFP expression plasmids were transfected in MLP29 cells. The cells were lysed, and total cell lysates analyzed by SDS-PAGE. Western blot analysis using an anti-GST– (top panel) and an anti-GFP (bottom panel) specific–antibody shows that the exogenous Mig6 and Cdc42* (arrowheads) are expressed at equal levels. Transfection of GFP expression plasmid was used as a negative control for the anti-GST and anti-GFP antibodies. Asterisk in panel D denotes an unspecific cross-reactive protein that is detected with anti-GST antibodies. Quantification of cell migration expressed as fold of induction over unstimulated cells in the presence of 10% FBS (E and G) or HGF (F and H). MLP29 cells were left untransfected or were transfected with the indicated GST-Mig6 expression plasmids (E and F)

We next addressed the relevance of the Mig6 CRIB domain, which had been suggested to bind the Rho family GTPase, Cdc42 (Makkinje et al., 2000). HGF activated Rho family GTPases in epithelial cells concomitant with cell-spreading responses, which was inhibited by dominant negative Cdc42 or Rac (Royal et al., 2000). Mig6 shares striking homology with the noncatalytic region of the cytoplasmic tyrosine kinase, activated Cdc42-associated tyrosine kinase (Ack), which interacts with Cdc42 by way of its CRIB domain and inhibits Cdc42's GTPase activity (Mott et al., 1999). Using the yeast two-hybrid assay, we first confirmed that full-length Mig6 bound Cdc42 with higher affinity than Rac (Fig. S2). We then asked if Mig6 would prevent the activation of Cdc42 in MLP29 cells. HGF stimulation of MLP29 led to an increase in the levels of GTP-bound Cdc42, as shown by pull-down experiments of transfected Cdc42 using the Ack-CRIB domain (Fig. 7 B). Cotransfection of Cdc42 with Mig6 essentially eliminated this effect (Fig. 7 B). We next investigated if the CRIB domain of Mig6 was essential for Mig6's inhibition of HGF-induced cell migration. We generated GST-tagged versions of Mig6 lacking the CRIB domain; a truncated NH_2-terminal fragment of Mig6 including the CRIB domain, but lacking the Ack homology domain; and the isolated CRIB domain only, and expressed them in MLP29 cells (Fig. 7 C). The mutant proteins were expressed at similar levels (Fig. 7 D) and in similar subcellular compartments (Fig. S2).

Next, we analyzed HGF-induced cell migration. $Mig6^{FL}$ inhibited cell migration twofold (Fig. 7 F). In contrast, Mig6 lacking the CRIB domain had no effect on HGF-induced cell migration (Fig. 7 F). The NH_2-terminal fragment of Mig6 including the CRIB domain and, more importantly, the isolated CRIB domain inhibited HGF-induced cell migration to the same extent as did $Mig6^{FL}$ (Fig. 7 F). The effects were specific for HGF-stimulated cells, because cell migration that was induced by FBS was not affected by ectopic expression of Mig6 including the CRIB domain, but lacking the Ack homology domain, or CRIB (Fig. 7 E). If the mechanism of Mig6 action involved the binding and inhibition of Cdc42, the coexpression of dominant-active Cdc42 (Cdc42*) may rescue the antimigratory effect of Mig6. To test this, we cotransfected MLP29 cells with $Mig6^{FL}$ and GFP or with the same amounts of $Mig6^{FL}$ and Cdc42* expression plasmids, and performed cell migration assays. The combination of $Mig6^{FL}$ and GFP led to an efficient block of migration, whereas the coexpression of $Mig6^{FL}$ and Cdc42* completely rescued cell migration. Expression of Cdc42* alone had no significant effect in this assay (Fig. 7 H). These results suggest that the CRIB domain of Mig6 is necessary and sufficient for inhibition of HGF-induced cell migration. They further suggest that part of Mig6's mechanism of action involves the regulation of Rho GTPases, such as Cdc42.

Discussion

The complex chain of events that attenuates signal transduction of receptor tyrosine kinases remains poorly understood. Recent studies revealed that negative receptor signaling involves intricate interactions between ubiquitin ligases, adaptor proteins, inhibitory proteins, cytoplasmic kinases, and phosphatases (Dikic and Giordano, 2003). Although some of these negative regulators can act on rather specific targets (protein tyrosine phosphatase inhibits insulin and insulin-like growth factor–1–stimulated signaling), others seem to inhibit multiple receptor tyrosine kinases (e.g., c-Cbl ubiquitin ligase) and generic signaling pathways. In this report, we show that Mig6 is induced by HGF in different cell lineages. Mig6 negatively regulates HGF/Met-mediated cellular responses, including cell migration and neurite growth. This suggests that Mig6 is part of a physiologic mechanism that negatively controls the strength and duration of Met signaling, thereby fine tuning signal transduction. Although further experiments are needed to clarify the exact mechanism of Mig6 action, our data suggest an important role for Mig6 interaction with Rho family GTPases.

Mig6 induction by external signals

We identified Mig6 in MLP29 cells as an RNA transcript that was induced highly by HGF and EGF and rather weakly by FGF2 and PDGF. Other investigators found that Mig6 was induced by serum, EGF and related ligands, and cellular stress factors (Wick et al., 1995; Makkinje et al., 2000; and references within). We have provided evidence that Met signaling is a major pathway for Mig6 expression in vivo by showing a reduction of *mig6* transcript levels in embryonic liver and lung of mouse mutants expressing a severe signaling hypomorph of Met (Fig. 1). We conclude that in many circumstances, Mig6 is expressed at low levels, and its expression is induced by HGF/Met signaling to activate feedback inhibition with some delay after the initiation of Met signaling. Consequently, the cell responds robustly to Met signaling, until Mig6 levels are high enough to attenuate the Met response. Alternatively, other external signals may have induced the expression of Mig6 before the cells were exposed to HGF, thereby reducing the cell's ability to respond to Met signaling. Loss of the ability to induce the expression of Mig6 may be part of the multiple step process toward malignancy. Consistent with this model, a recent large-scale expression profiling study noted that Mig6 expression was down-regulated in patients who had breast cancer with short survival time (Amatschek et al., 2004). It seems as if loss of Mig6 provides a growth advantage and perhaps metastatic potential for breast cancer cells.

or cotransfected with a combination of GFP-Cdc42* and GST-$Mig6^{FL}$ expression plasmids as indicated (G and H) and seeded onto the upper compartment of the Boyden chamber. The NH_2-terminal half of Mig6 ($Mig6^{NT}$) and its CRIB domain ($Mig6^{CRIB}$) were able to inhibit HGF-mediated migration significantly compared with control cells (for both $P = 0.001$, *t* test) (panel F). **, $P < 0.01$. In contrast, $Mig6^{\Delta CRIB}$ was not able to reduce HGF-mediated migration significantly compared with untransfected control ($P = 0.88$, *t* test). The inhibition of HGF-mediated migration due to GST-$Mig6^{FL}$ expression was rescued significantly by the coexpression of GFP-Cdc42* ($P = 0.76$), but not of GFP expression plasmids (average of three separate experiments; $P < 0.0001$). 10% FBS-induced cell migration was not affected by any of the Mig6-expressing constructs (E and G).

Mig6 modulates a variety of cellular responses

Previous work showed that Mig6 inhibits cell proliferation downstream of ErbB family receptors (Fiorentino et al., 2000; Hackel et al., 2001; Anastasi et al., 2003). This includes studies in which Mig6 was silenced by RNA interference, and provided first evidence for its role as an endogenous inhibitor of EGFR-mediated proliferation (Anastasi et al., 2005; Xu et al., 2005). Until now, the role of Mig6 in ErbB-mediated cell migration had not been addressed. However, this is an important question; numerous studies demonstrated that EGF and related ligands for EGFR/ErbB receptors stimulate chemotactic migration in vertebrate and invertebrate systems (Wells and Lillien, 2004). Our study has concentrated on the role of Mig6 in Met-mediated cell migration, a process that is implicated in several physiologic contexts, including myoblast migration during development, scattering and branching morphogenesis of epithelial cells, and neuronal migration in the developing forebrain (Powell et al., 2001; Birchmeier et al., 2003; Rosario and Birchmeier, 2003). Met signaling also is critical for neurite extension and branching of different neuronal subpopulations (Maina and Klein, 1999; Thompson et al., 2004), a process that has similarities with invasive growth of malignant cells (Trusolino and Comoglio, 2002). We found that Mig6 overexpression effectively and specifically reduced HGF-induced migration of a cell line of hepatic origin and of primary cortical neurons. Mig6 also effectively blocked HGF-induced neurite growth of primary sympathetic neurons. In converse experiments, *mig6* knock-down effectively enhanced cell migration of hepatic progenitor cells and mildly, yet significantly, enhanced neurite growth of sympathetic neurons.

Mig6 acts distally from Met by way of interaction with Rho family GTPases

Mig6 is a multiadaptor molecule whose amino-terminal 38 amino acid residues show homologies with the conserved CRIB domain that is present in a variety of intracellular signaling molecules (Pirone et al., 2001). Mig6 contains putative binding sites for SH3-containing molecules such as Grb2, PI3K, and PLCγ (Fiorentino et al., 2000), and for 14–3-3 and PDZ-domain containing proteins. Notably, Mig6 includes a COOH-terminal region that is highly homologous to the noncatalytic portion of Ack1. A region within this Ack1 homology domain was identified as an EGFR-binding motif (Fiorentino et al., 2000; Anastasi et al., 2003) that was necessary and sufficient for the inhibition of EGFR signaling (Xu et al., 2005). Expression of Mig6/receptor-associated late transducer in tumor cells modestly reduced the levels of ErbB-mediated phospho-MAPK and phospho-Akt expression, which suggested some interference with mitogenic signaling pathways (Anastasi et al., 2005). Conversely, loss of Mig6 led to sustained MAPK phosphorylation in EGF-stimulated keratinocytes (Ballaro et al., 2005 and unpublished data). The association between Mig6 and Met by way of Grb2 interaction (Fig. 7) suggests the possibility that Mig6 inhibits Met signaling in a receptor-proximal fashion. However, we have been unable to detect changes in the levels of Met-mediated phospho-MAPK and phospho-Akt expression in cells that transiently overexpress Mig6 (Fig. S2). Therefore, we favor the view that the antimigratory effect of Mig6 in MLP29 cells involves other pathways.

Because the CRIB domain of Mig6 binds Cdc42 in a GTP-dependent manner (Makkinje et al., 2000 and this report), HGF stimulation activates Cdc42, and activated Cdc42 is required for HGF-induced lamellipodia formation and cell movement (Royal et al., 2000), we favor the possibility that Mig6 inhibits Cdc42-mediated cell movement by way of its CRIB domain. In support of this hypothesis, we show that (i) overexpression of a Mig6 construct lacking the CRIB domain, but retaining Grb2-binding capabilities, is unable to suppress HGF-induced migration; (ii) overexpression of the Mig6 CRIB domain alone is sufficient to inhibit HGF-induced migration; and (iii) coexpression of Mig6 with a dominant-active form of Cdc42 rescues the antimigratory effects of Mig6. Therefore, the mechanism of Mig6 inhibition of Met resembles the mechanism of Ack1 inhibition of EGFR. The *Caenorhabditis elegans* orthologue of Ack1, Ark, associates with EGFR by way of binding to Sem5, the *C. elegans* orthologue of Grb2 (for review see Worby and Margolis, 2000). Similar to Mig6, overexpression of the CRIB domain of Ack1 is sufficient to inhibit growth factor–induced activation of Cdc42 (Nur-E-Kamal et al., 1999). Furthermore, overexpression of the CRIB domain of another small GTPase-binding protein, PAK (an effector of Rac1), by way of its interaction with Rac1, inhibits Semaphorin 3A-induced growth cone collapse (Vastrik et al., 1999). Together, these results indicate that CRIB domains are sufficient to inhibit the biologic effects of specific GTPases.

We propose that Mig6 is part of a network of negative signaling molecules that fine tune and attenuate Met and ErbB signaling in development and disease. The analysis of *mig6* mutant mice provided genetic evidence for a role of Mig6 in the maintenance of joints and cartilage (Zhang et al., 2005) and in skin morphogenesis and cancer (unpublished data). They will be an invaluable tool in our efforts to elucidate the inhibitory functions and molecular interactions of Mig6 in the context of an intact tissue.

Materials and methods

Mouse 15,000 cDNA microarray production and data analysis

The "NIA mouse 15k cDNA microarray" chip production, isolation of RNA, labeling of cDNA probes, and hybridization to the cDNA array was performed as described (Cortes-Canteli et al., 2004). In brief, the hybridization was performed in duplicate using total RNA samples that were extracted from two independent batches of cultured cells. Stimulated and mock-treated samples were labeled by Cy-5 and Cy-3-dUTP, respectively. Data acquisition and initial data analysis were performed with GenePix Pro 3.0, and data tables were analyzed further in Microsoft Excel to obtain the gene list. Quality control was performed by eye to confirm scanner alignment and absence of significant bubbles and scratches. Scatter plots were used further to eliminate the unacceptable hybridization data. GenePix Pro program calculates the normalization factor of each hybridization, based on the premise that the arithmetic mean of the ratios from every feature on the given array should be equal to 1. Therefore, normalization was performed by multiplying the factor to ratio of medians (ROM) in each gene. The genes that passed all of these criteria were sorted first by sum of median (SOM), which indicates the intensity of hybridization. To obtain the list of genes that are relatively abundant, the genes that showed more than 5,000 of SOM were selected. Finally, the genes were sorted by ROM. The genes that showed more than ± 1.8-fold changes were selected in the data table from each hybridization. Finally, the data were compared between the two hybridizations and average ROM was calculated. Gene functions were categorized

based on the information given in the NIA mouse 15k cDNA clone gene ID list at the first instance and modified when necessary.

Northern blots
Total RNA was extracted from different cell lines in various experimental conditions using the RNAClean Solution (Hybaid). 20 μg total RNA was electroporated and blotted onto Genescreen nylon membrane (NEN Life Science Products). Labeled probes were generated using random primers and hybridized (6× SSC, 5× Denhardt solution, and 100 μg salmon sperm DNA) with the membrane for 18 h at 65°C. cDNA inserts used as probes were obtained by NotI/SalI double restriction digestion of the NIA mouse 15k cDNA clones.

RNA interference
siRNA oligonucleotides (first set [AAGGUCAAGCUUGCCCCCUC-dTdT] and second set [GAGGAUCAAGUUAUGUGUGG-dTdT]) were designed and used for cell transfections as described (Elbashir et al., 2001). Sense and anti-sense siRNA oligonucleotides (DARMAKOM) were diluted in annealing buffer (100 mM K-Acetate, 30 mM Hepes-KOH, 2 mM Mg-Acetate) to the final concentration of 20 μM, denatured for 1 min at 90°C, and annealed by incubation for 1 h at 37°C. 6 μl siRNA duplex was transfected into 4×10^4 cells using oligofectamine (Invitrogen), according to the manufacturer's instructions. After transfection, cells were left in Dulbecco's minimum essential medium (DMEM) plus 0.1% FBS for 72 h and transfected a second time with the same siRNA duplex. The aphidicolin treatment was performed as described above. 24 h after the second transfection, cells were harvested and plated on the upper face of the Boyden chamber as described above.

Plasmids and expression vectors
Primer sequences are available upon request. The V5 COOH-terminal, GST NH_2-terminal, and His COOH-terminal tagged Mig6 full-length and mutant proteins were generated using the Gateway Cloning technology according to the manufacturer's instructions (Invitrogen). In brief, Mig6 full-length and deletion mutants were amplified by PCR from the IRAK clone IRAKp961F0910 using oligonucleotides that contained the minimal recombination sequences (5′-ATTB1 and 3′-ATTB2). PCR amplified products were recombined into pDONOR201 vector by the use of a mixture of recombination proteins that was provided by the manufacturer. The pDONOR201 vectors containing Mig6 full-length or deletion mutants were shuttled into pCDNA 6.2 COOH-terminal-V5, pDEST 27 NH_2-terminal-GST, and pDEST26 NH_2-terminal-His plasmids (all Invitrogen) for mammalian expression or into pDest15 N-term-GST for bacterial expression. The LacZ-V5 expression plasmid was purchased (Invitrogen). GFP-$Cdc42^{WT}$ and dominant active expression plasmids were provided by M. Way. The CRIB domain of Ack was amplified by PCR from the I.M.A.G.E. Consortium cDNA Clones (Clone ID IMAGp998I1013902Q3) (Lennon et al., 1996) and was subcloned into pCRII-TOPO cloning vector (Invitrogen) following the manufacturer's instructions. The fragment was inserted into the pFAT2 vector for bacterial expression. The pGEX-NH_2-terminal-GST-Mig6, containing the Mig6 COOH-terminal half (from aa 273 to 459), was provided by A. Ullrich and was used to produce the Mig6 antigen.

Primary cortical neuron culture, cell migration assays, and growth factors
MLP29 cells were cultured and transiently transfected as described (Muller et al., 2002). C2C12 were grown as described (Yaffe and Saxel, 1977). Primary hepatocytes were cultured as described (Maina et al., 2001). The transwell assay was performed as described previously (de Luca et al., 1999). In brief, 10^5 MLP29 cells were seeded on the upper face of the Boyden chamber membrane (8 μm pore; Costar), which was coated previously with 0.15 $\mu g/cm^2$ of fibronectin (Sigma-Aldrich). The cells were stimulated with 40 ng/ml of hepatocyte growth factor (HGF) (R&D Systems), 10 ng/ml EGF, 30 ng/ml PDGF (Sigma-Aldrich), 25 ng/ml fibroblast growth factor 2 (FGF2; Sigma-Aldrich), and 100 ng/ml SDF-1 (Calbiochem). To assay cell migration in the absence of cell proliferation, cells were treated for 24 h before and during the migration assay with DMSO-(Fluka) or 1.6 μg/ml aphidicolin-containing media (Sigma-Aldrich).

Cortical neurons were obtained by digestion of E15.5 mouse telencephalon for 15 min at 37°C with trypsin-EDTA (GIBCO BRL). The neurons were washed twice with DMEM-F12 supplemented with 10% horse serum (GIBCO BRL), washed once in neurobasal medium containing B27 supplement (NB/B27, 50:1, GIBCO BRL) and were dissociated with a fire-polished glass Pasteur pipette. Cortical neurons were dissected and electroporated by mixing 6×10^5 cells with 24 μg expression plasmid, transferred into an electroporation cuvette (MBP Molecular Bioproducts), and electroporated (five pulses at 270 V of 3 msec separated by 1-s interval) using the Electrosquare porator (ECM830, BTX). The cells were incubated for 10 min at 4°C. 10^5 cells were seeded on the upper side of the Boyden chamber (5-μm pore, Costar), which was coated previously with poly-D-ornithin (Sigma-Aldrich). 3 h later, the appropriate growth factors were added to the lower compartment for 18 h. The cells were fixed with 4% PFA (Merck) for 30 min at room temperature and incubated for 10 min at 4°C. Boyden chamber filters were mounted onto glass coverslips in the presence of vectashield/DAPI (Vector Laboratories). The cells were analyzed directly under a Zeiss Axiophot fluorescent microscope.

In situ hybridization and biochemistry
In situ hybridizations and preparations of probes were performed as described (Helmbacher et al., 2003). Mig6 sense and anti-sense probes were obtained by NotI and SalI restriction digests of the NIA clone h3011f08. The met in situ probe was described previously (Helmbacher et al., 2003). Immunoblotting and immunocytochemistry were performed as described (Maina et al., 2001). Recombinant GST-Mig6 fusion proteins were purified according to standard procedures. MLP29 cell lysates were incubated for 1 h at 4°C with recombinant proteins that were immobilized on glutathione-sepharose. The glutathione-sepharose beads were washed several times in cell lysis buffer, eluted with sample buffer, and analyzed by immunoblotting.

Antibodies
The rabbit anti-Mig6 antibody was generated as described previously (Hackel et al., 2001). The anti-phospho-MAPK, anti-MAPK, and anti-phospho-Akt (New England Biolabs, Inc.) antibodies were used as described previously (Maina et al., 2001). Antibody dilutions: monoclonal anti-tubulin (Sigma-Aldrich) 1:2,000 for Western blot (WB) analysis; monoclonal anti-V5 (Invitrogen) 1:1,000 and 1:250 for WB and immunocytochemical (IC) analysis, respectively; rabbit polyclonal anti-Met (BIOMOL Research Laboratories) and anti-GST (Santa Cruz Biotechnology, Inc.) 1:500 for WB analysis; anti–microtubule-associated protein 2 (Sigma-Aldrich) 1:10,000 for IC analysis; monoclonal anti-Grb2 (Transduction Labs) 1:1,000 for WB analysis; donkey polyclonal anti–mouse Alexa488 (Molecular Probes) and anti–rabbit CY3 (Jackson ImmunoResearch Laboratories) 1:200 for IC analysis; and polyclonal goat anti–mouse and anti–rabbit HRP-conjugated (GE Healthcare) 1:2,000 for WB analysis.

Imaging
All cell images were obtained with an Axioplan-2 imaging fluorescent microscope (Carl Zeiss MicroImaging, Inc.) equipped with a RT Slider 2.3.1 digital color camera (Diagnostic Instruments). A 40× objective was used, except for the in situ hybridization images that were taken with a 20× lens (Carl Zeiss MicroImaging, Inc.).

Yeast two-hybrid system
The NH_2-terminal half of Mig6 and the CRIB domain of PAK and Ack were inserted by way of BamHI/XhoI into the yeast two-hybrid prey vector pAct2. $Cdc42^{WT}$ and Rac^{WT} were inserted by way of BamHI/SalI into the pGBT9 bait vector. These plasmids were transformed in the indicated combination into the reporter strain PJ69-4A according to the CLONTECH Laboratories yeast protocol handbook. The double transformants were selected by plating onto synthetic media lacking leucine and tryptophane with 2% glucose as the carbon source (Leu−/Trp−). Double transformants were restreaked onto Leu−/Trp− or synthetic media lacking leucine, tryptophan, histidine, and adenine (quadruple drop out).

Recombinant protein purification and Cdc42 activation assay
Recombinant GST fusion proteins were purified according to standard procedures. MLP29 cell lysates were incubated for 1 h at 4°C with recombinant proteins immobilized on glutathione-sepharose. The glutathione-sepharose beads were washed several times in cell lysis buffer, eluted with sample buffer, and analyzed by immunoblotting. For the Cdc42 activation assay, MLP29 cells in various experimental conditions were lysed (50 mM Tris-Cl pH 7.4, 5 mM $MgCl_2$, 200 mM NaCl, 1 mM sodium orthovanadate, 1% NP-40, 10% glycerol, and a mixture of protease inhibitors EDTA-free), and the lysates were incubated with the recombinant GST-Ack-CRIB protein bound to glutathione-sepharose beads for 1.5 h at 4°C. The proteins were eluted from the beads, and analyzed by SDS-PAGE and immunoblotting.

Paravertebral sympathetic neuron cultures
Superior cervical ganglia were dissected from postnatal day 40 (P40) CD1 mice. Neuron cultures were set up as described (Thompson et al., 2004). HGF stimulation and quantification of neuronal survival was done

as described (Thompson et al., 2004). Sholl analysis was performed as described previously (Sholl, 1953). For protein extraction, primary cultures of dissociated P40 superior cervical ganglion neurons were grown for 3–6 h in culture before being stimulated for different times with HGF. Cells were harvested and homogenized as described above.

Online supplemental material

Fig. S1 shows Northern blot analysis of selected genes from the gene list. Fig. S2 shows the effects of Mig6 on canonical Met signaling, yeast two-hybrid interactions between Mig6 and Cdc42/Rac, and immunohistochemical analysis of overexpressed and endogenous Mig6. Table S1 and Table S2 list the genes that are regulated by HGF in MLP29 cells. Online supplemental material available at http://www.jcb.org/cgi/content/full/jcb.200502013/DC1.

We thank R. Sanchez and W. Ansorge for technical help; M. Casenghi, J. Egea, F. Helmbacher, A. Ullrich, and B. Short for scientific discussions and intellectual input; and A. Ullrich (Max Planck Institute for Biochemistry, Martinsried, Germany), M. Way (Cancer Research UK, London, UK), and A. Moumen (Developmental Biology Institute of Marseille, Marseille, France) for reagents.

This work was supported by the Max-Planck Society and by additional grants from the Wellcome Trust (to A.M. Davies) and Boehringer Ingelheim (to R. Klein).

Submitted: 2 February 2005
Accepted: 19 September 2005

References

Amatschek, S., U. Koenig, H. Auer, P. Steinlein, M. Pacher, A. Gruenfelder, G. Dekan, S. Vogl, E. Kubista, K.H. Heider, et al. 2004. Tissue-wide expression profiling using cDNA subtraction and microarrays to identify tumor-specific genes. *Cancer Res.* 64:844–856.

Anastasi, S., L. Fiorentino, M. Fiorini, R. Fraioli, G. Sala, L. Castellani, S. Alema, M. Alimandi, and O. Segatto. 2003. Feedback inhibition by RALT controls signal output by the ErbB network. *Oncogene.* 22:4221–4234.

Anastasi, S., G. Sala, C. Huiping, E. Caprini, G. Russo, S. Iacovelli, F. Lucini, S. Ingvarsson, and O. Segatto. 2005. Loss of RALT/MIG-6 expression in ERBB2-amplified breast carcinomas enhances ErbB-2 oncogenic potency and favors resistance to Herceptin. *Oncogene.* 24:4540–4548.

Ballaro, C., S. Ceccarelli, C. Tiveron, L. Tatangelo, A.M. Salvatore, O. Segatto, and S. Alema. 2005. Targeted expression of RALT in mouse skin inhibits epidermal growth factor receptor signalling and generates a waved-like phenotype. *EMBO Rep.* 6:755–761.

Birchmeier, C., W. Birchmeier, E. Gherardi, and G.F. Vande Woude. 2003. Met, metastasis, motility and more. *Nat. Rev. Mol. Cell Biol.* 4:915–925.

Cortes-Canteli, M., M. Wagner, W. Ansorge, and A. Perez-Castillo. 2004. Microarray analysis supports a role for ccaat/enhancer-binding protein-beta in brain injury. *J. Biol. Chem.* 279:14409–14417.

de Luca, A., N. Arena, L.M. Sena, and E. Medico. 1999. Met overexpression confers HGF-dependent invasive phenotype to human thyroid carcinoma cells in vitro. *J. Cell. Physiol.* 180:365–371.

Dikic, I., and S. Giordano. 2003. Negative receptor signalling. *Curr. Opin. Cell Biol.* 15:128–135.

Elbashir, S.M., J. Harborth, W. Lendeckel, A. Yalcin, K. Weber, and T. Tuschl. 2001. Duplexes of 21-nucleotide RNAs mediate RNA interference in cultured mammalian cells. *Nature.* 411:494–498.

Fiorentino, L., C. Pertica, M. Fiorini, C. Talora, M. Crescenzi, L. Castellani, S. Alema, P. Benedetti, and O. Segatto. 2000. Inhibition of ErbB-2 mitogenic and transforming activity by RALT, a mitogen-induced signal transducer which binds to the ErbB-2 kinase domain. *Mol. Cell. Biol.* 20:7735–7750.

Fiorini, M., C. Ballaro, G. Sala, G. Falcone, S. Alema, and O. Segatto. 2002. Expression of RALT, a feedback inhibitor of ErbB receptors, is subjected to an integrated transcriptional and post-translational control. *Oncogene.* 21:6530–6539.

Hackel, P.O., M. Gishizky, and A. Ullrich. 2001. Mig-6 is a negative regulator of the epidermal growth factor receptor signal. *Biol. Chem.* 382:1649–1662.

Helmbacher, F., E. Dessaud, S. Arber, O. deLapeyriere, C.E. Henderson, R. Klein, and F. Maina. 2003. Met signaling is required for recruitment of motor neurons to PEA3-positive motor pools. *Neuron.* 39:767–777.

Labouesse, M. 2004. Epithelium-mesenchyme: a balancing act of RhoGAP and RhoGEF. *Curr. Biol.* 14:R508–510.

Lennon, G., C. Auffray, M. Polymeropoulos, and M.B. Soares. 1996. The I.M.A.G.E. Consortium: an integrated molecular analysis of genomes and their expression. *Genomics.* 33:151–152.

Maina, F., and R. Klein. 1999. Hepatocyte growth factor, a versatile signal for developing neurons. *Nat. Neurosci.* 2:213–217.

Maina, F., F. Casagranda, E. Audero, A. Simeone, P.M. Comoglio, R. Klein, and C. Ponzetto. 1996. Uncoupling of Grb2 from the Met receptor in vivo reveals complex roles in muscle development. *Cell.* 87:531–542.

Maina, F., G. Pante, F. Helmbacher, R. Andres, A. Porthin, A.M. Davies, C. Ponzetto, and R. Klein. 2001. Coupling Met to specific pathways results in distinct developmental outcomes. *Mol. Cell.* 7:1293–1306.

Makkinje, A., D.A. Quinn, A. Chen, C.L. Cadilla, T. Force, J.V. Bonventre, and J.M. Kyriakis. 2000. Gene 33/Mig-6, a transcriptionally inducible adapter protein that binds GTP-Cdc42 and activates SAPK/JNK. A potential marker transcript for chronic pathologic conditions, such as diabetic nephropathy. Possible role in the response to persistent stress. *J. Biol. Chem.* 275:17838–17847.

Medico, E., A.M. Mongiovi, J. Huff, M.A. Jelinek, A. Follenzi, G. Gaudino, J.T. Parsons, and P.M. Comoglio. 1996. The tyrosine kinase receptors Ron and Sea control "scattering" and morphogenesis of liver progenitor cells in vitro. *Mol. Biol. Cell.* 7:495–504.

Mott, H.R., D. Owen, D. Nietlispach, P.N. Lowe, E. Manser, L. Lim, and E.D. Laue. 1999. Structure of the small G protein Cdc42 bound to the GTPase-binding domain of ACK. *Nature.* 399:384–388.

Muller, M., A. Morotti, and C. Ponzetto. 2002. Activation of NF-kappaB is essential for hepatocyte growth factor-mediated proliferation and tubulogenesis. *Mol. Cell. Biol.* 22:1060–1072.

Nur-E-Kamal, M.S., J.M. Kamal, M.M. Qureshi, and H. Maruta. 1999. The CDC42-specific inhibitor derived from ACK-1 blocks v-Ha-Ras-induced transformation. *Oncogene.* 18:7787–7793.

Pirone, D.M., D.E. Carter, and P.D. Burbelo. 2001. Evolutionary expansion of CRIB-containing Cdc42 effector proteins. *Trends Genet.* 17:370–373.

Powell, E.M., W.M. Mars, and P. Levitt. 2001. Hepatocyte growth factor/scatter factor is a motogen for interneurons migrating from the ventral to dorsal telencephalon. *Neuron.* 30:79–89.

Prunotto, C., T. Crepaldi, P.E. Forni, A. Ieraci, R.G. Kelly, S. Tajbakhsh, M. Buckingham, and C. Ponzetto. 2004. Analysis of Mlc-lacZ Met mutants highlights the essential function of Met for migratory precursors of hypaxial muscles and reveals a role for Met in the development of hyoid arch-derived facial muscles. *Dev. Dyn.* 231:582–591.

Rosario, M., and W. Birchmeier. 2003. How to make tubes: signaling by the Met receptor tyrosine kinase. *Trends Cell Biol.* 13:328–335.

Royal, I., N. Lamarche-Vane, L. Lamorte, K. Kaibuchi, and M. Park. 2000. Activation of cdc42, rac, PAK, and rho-kinase in response to hepatocyte growth factor differentially regulates epithelial cell colony spreading and dissociation. *Mol. Biol. Cell.* 11:1709–1725.

Sholl, D.A. 1953. Dendritic organization in the neurons of the visual and motor cortices of the cat. *J. Anat.* 87:387–406.

Tanaka, T.S., S.A. Jaradat, M.K. Lim, G.J. Kargul, X. Wang, M.J. Grahovac, S. Pantano, Y. Sano, Y. Piao, R. Nagaraja, et al. 2000. Genome-wide expression profiling of mid-gestation placenta and embryo using a 15,000 mouse developmental cDNA microarray. *Proc. Natl. Acad. Sci. USA.* 97:9127–9132.

Thompson, J., X. Dolcet, M. Hilton, M. Tolcos, and A.M. Davies. 2004. HGF promotes survival and growth of maturing sympathetic neurons by PI-3 kinase- and MAP kinase-dependent mechanisms. *Mol. Cell. Neurosci.* 27:441–452.

Trusolino, L., and P.M. Comoglio. 2002. Scatter-factor and semaphorin receptors: cell signalling for invasive growth. *Nat. Rev. Cancer.* 2:289–300.

Vastrik, I., B.J. Eickholt, F.S. Walsh, A. Ridley, and P. Doherty. 1999. Sema3A-induced growth-cone collapse is mediated by Rac1 amino acids 17-32. *Curr. Biol.* 9:991–998.

Wells, A., and L. Lillien. 2004. Attraction or repulsion: a matter of individual taste? *Sci. STKE.* 2004:pe47.

Wick, M., C. Burger, M. Funk, and R. Muller. 1995. Identification of a novel mitogen-inducible gene (mig-6): regulation during G1 progression and differentiation. *Exp. Cell Res.* 219:527–535.

Worby, C., and B. Margolis. 2000. Positive versus negative signaling of LET-23: regulation through the adaptor protein, SEM-5. *Sci. STKE.* 2000:PE2.

Xu, D., A. Makkinje, and J.M. Kyriakis. 2005. Gene 33 is an endogenous inhibitor of epidermal growth factor (EGF) receptor signaling and mediates dexamethasone-induced suppression of EGF function. *J. Biol. Chem.* 280:2924–2933.

Yaffe, D., and O. Saxel. 1977. A myogenic cell line with altered serum requirements for differentiation. *Differentiation.* 7:159–166.

Zhang, Y.W., Y. Su, N. Lanning, P.J. Swiatek, R.T. Bronson, R. Sigler, R.W. Martin, and G.F. Vande Woude. 2005. Targeted disruption of Mig-6 in the mouse genome leads to early onset degenerative joint disease. *Proc. Natl. Acad. Sci. USA.* 102:11740–11745.